Electronic Supplementary Material (ESI) for Physical Chemistry Chemical Physics.

Figures

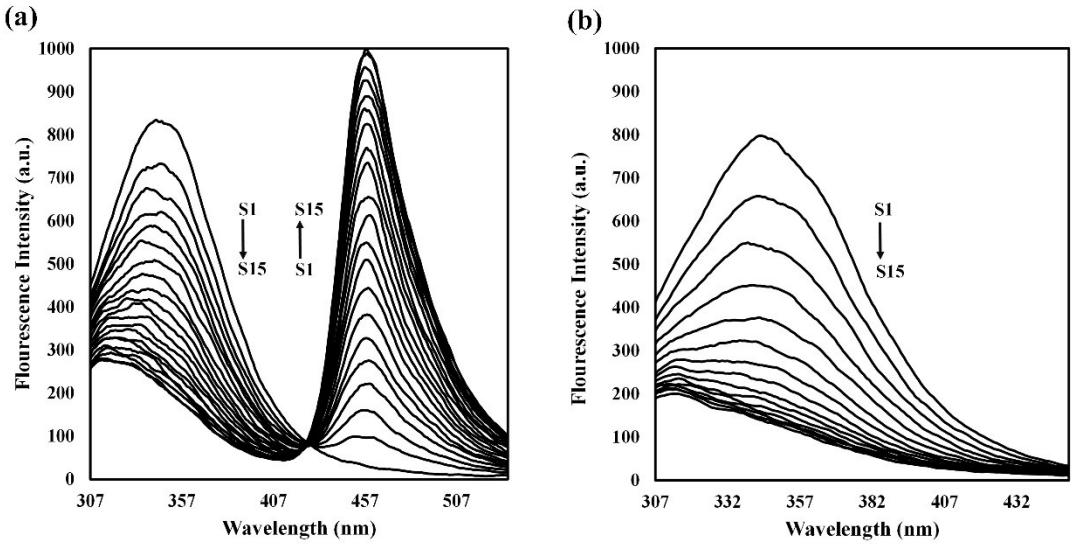

Figure S1: emission spectra of HSA with various concentration of DAC (a) and BAC (b) at 298 K. Flouresence spectra Arrows (S1-S15) indicate the trend from lowest (0 μM) to highest (1.33 μM).

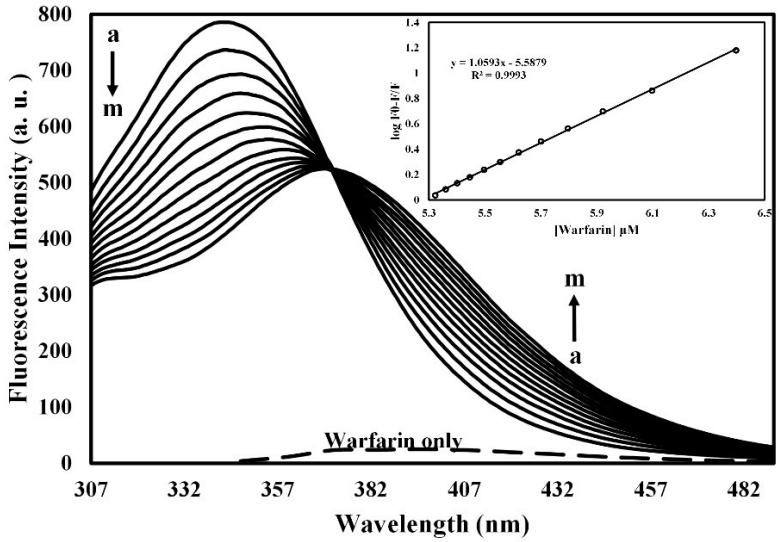

Figure S2: emission spectra of HSA with various concentration of warfarin at 298 K. Arrows (A-m) indicate the trend from lowest (0 μM) to highest (4.8 μM). Best linear plot of log F_0-F/F versus log [warfarin] according to Eq. 3. at temperature of 298 K. The slopes and vertical intercepts were used to calculation of (n = 1) and ($K_a = 3.87 \times 10^5$ mol L^{-1}) respectively.

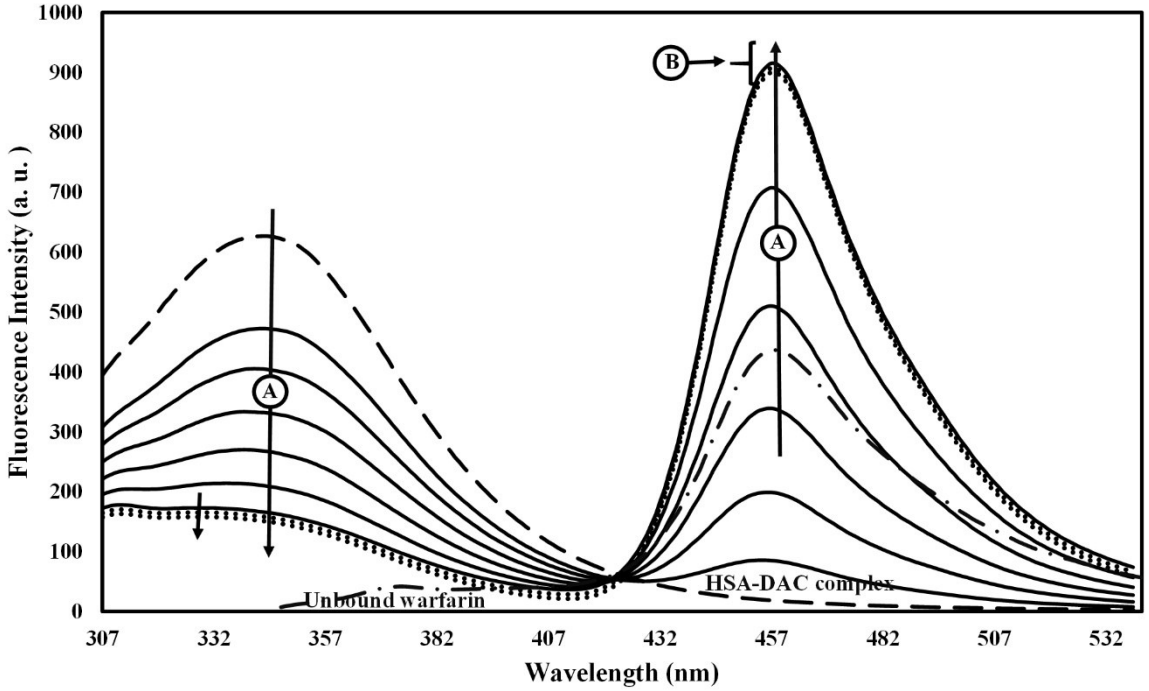

Figure S3: Fluorescence spectra of HSA, DAC:HSA binary mixture and DAC:HSA:WAR ternary mixture in phosphate buffer of pH 7.0 at 298 K (λ_{ex} = 280 nm). Dashed curve shows HSA in the concentration of 1.36 μM, solid curves show the HSA-DAC binary mixture in the molar ratio of [DAC]/[HSA]= 0, 0.3, 0.4, 0.5, 0.6, 0.7 and 0.9 and dotted curves show WAR-HSA-DAC ternary mixture in the molar ratio of [WAR]: [HSA]: [DAC]= 0.9: 1: 0.9, 1.8: 1: 0.9 and 2.6: 1: 0.9. Blue curve shows the unbound warfarin in 390 nm and HSA-DAC complex in 457 nm (λ_{ex} = 330 nm).

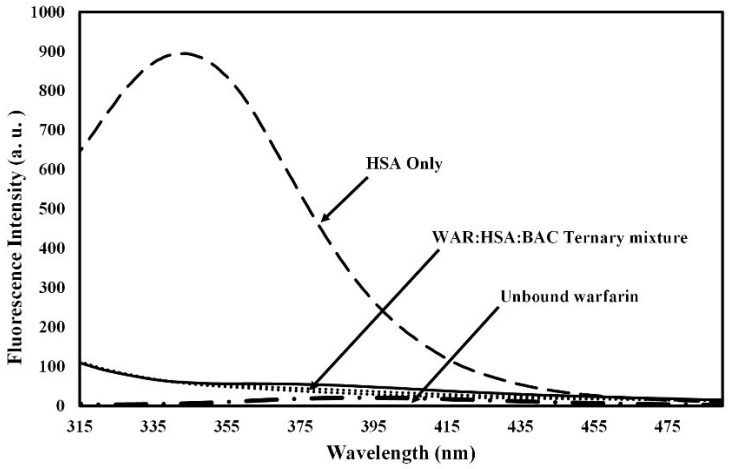

Figure S4: Fluorescence spectra of HSA, BAC:HSA binary mixture and BAC:HSA:WAR ternary mixture in phosphate buffer of pH 7.0 at 298 K (λ_{ex} = 280 nm). Dashed curve shows

HSA in the concentration of 1.36 μM, solid curve shows the HSA-BAC binary mixture in the molar ratio of [BAC]/[HSA]= 0.9 and dotted curves show WAR-HSA-BAC ternary mixture in the molar ratio of [WAR]: [HSA]: [BAC]= 0.9: 1: 0.9, 1.8: 1: 0.9 and 2.6: 1: 0.9. Blue curve shows the unbound warfarin in 390 nm and HSA-BAC complex in 457 nm (λ_{ex} = 330 nm).

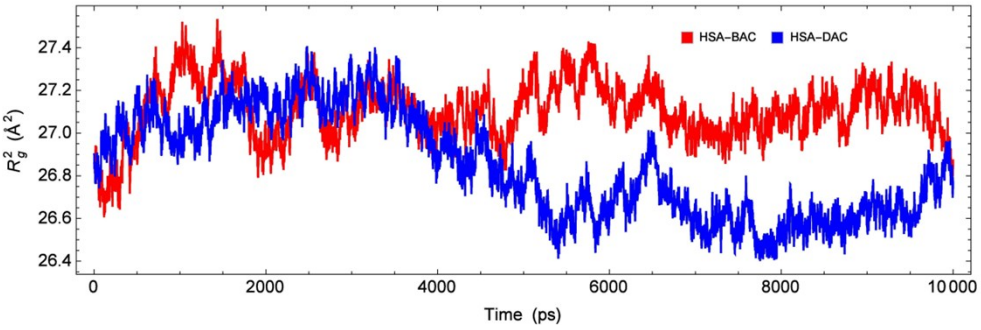

Figure S5. Time dependence of radius of gyration of protein over MD trajectories.

Tables

Table S1: Changes in the secondary structure of HSA in the absence and presence of various concentrations of DAC at 298 K.

	HSA	**DAC**	**BAC**	**DAC**	**BAC**	**DAC**	**BAC**
	(1.45 μM)	(0.96μM)		(1.92μM)		(2.88 μM)	
%Helix	65.9	65	63.96	64.6	63.94	64.1	63.65
% Beta-Sheet	18.9	19.2	19.64	19.3	19.44	19.6	19.73
% Rndm. Coil	15.2	15.8	16.4	16.1	16.62	16.3	16.62

Table S2. Different parameters obtained from SVD to determine number factors (significant components) in fluorescence spectra of HSA/DAC and HSA/BAC.

	DAC				BAC			
factors	**eig**	**log(eig)**	**REV**	**RSD**	**eig**	**log(eig)**	**REV**	**RSD**
1	8.68	0.94	4.99	475.30	8.42	0.93	4.84	63.85
2[a]	7.98	0.90	4.31	21.06	**6.19**	**0.79**	**2.64**	**1.53**
3[b]	**5.14**	**0.71**	**1.50**	**10.83**	2.66	0.42	-0.86	1.06
4	3.96	0.60	0.35	9.77	1.94	0.29	-1.56	0.95
5	3.89	0.59	0.31	8.76	1.89	0.28	-1.58	0.83
6	3.74	0.57	0.18	7.99	1.80	0.25	-1.64	0.73
7	3.71	0.57	0.18	7.18	1.59	0.20	-1.82	0.66
8	3.62	0.56	0.12	6.46	1.54	0.19	-1.83	0.58

[a] Optimum number of components in HSA-BAC system

[b] Optimum number of components in HSA-DAC system

Table S3. High affinity members of Warfarin-HSA complex ensemble obtained from docking in drug site 1. Only the results of up to 1 kcal/mol higher than the best affinity were reported here. All RMSD values are calculated for docked ligand with respect to its predicted pose in 2BXD.

PDB ID	Affinity	RMSD	PDB ID	Affinity	RMSD	PDB ID	Affinity	RMSD
2BXD	-9.6	0.00	2I30	-9.0	0.94	2BXP	-8.8	2.33
4IW2	-9.5	0.40	2BXB	-9.0	0.79	2XSI	-8.8	2.40
1E7E	-9.3	0.71	1E7G	-9.0	0.98	3B9L	-8.8	1.05
2BXC	-9.3	1.09	3LU6	-9.0	2.33	3SQJ	-8.8	0.56

1AO6	-9.2	0.97	1BKE	-8.9	1.16	4L9Q	-8.7	0.58
1BM0	-9.2	0.92	3B9M	-8.9	2.37	1H9Z	-8.7	2.26
1E7F	-9.2	2.50	2BXI	-8.8	2.32	4L8U	-8.7	0.90
4K2C	-9.1	0.98	1HA2	-8.8	0.47	1GNJ	-8.7	1.07
1BJ5	-9.1	1.03	2BX8	-8.8	2.20	2XVV	-8.7	0.75

Table S4. High affinity members of DAC-HSA complex ensemble obtained from docking in drug site 1. Only the results of up to 1 kcal/mol higher than the best affinity were reported here. All RMSD values are calculated for docked ligand with respect to its predicted pose in 4IW2.

PDB ID	Affinity	RMSD	PDB ID	Affinity	RMSD	PDB ID	Affinity	RMSD
4IW2	-9.9	0.00	4G03	-9.3	0.54	2XVV	-9.1	0.70
4EMX	-9.9	0.35	2BXM	-9.3	1.43	2BXH	-9.1	1.13
4L8U	-9.7	0.72	4LB2	-9.3	0.53	2BXQ	-9.1	1.79
2I30	-9.6	1.75	2BXN	-9.3	1.19	2BXB	-9.1	1.77
3LU6	-9.5	1.87	1E7H	-9.3	2.33	2BXK	-9.1	1.38
3LU7	-9.5	1.55	1E7E	-9.2	1.61	2BXI	-9.0	1.56
1HK5	-9.5	2.42	4L9K	-9.2	1.01	1BJ5	-9.0	1.65
2BXD	-9.4	1.77	1N5U	-9.1	1.43	1E7A	-9.0	1.61
3JRY	-9.3	0.91	1GNJ	-9.1	1.74	1GNI	-2.4	2.4

Table S5. High affinity members of BAC-HSA complex ensemble obtained from docking in drug site 1. Only the results of up to 1 kcal/mol higher than the best affinity were reported here. All RMSD values are calculated for docked ligand with respect to its predicted pose in 4IW2.

PDB ID	Affinity	RMSD	PDB ID	Affinity	RMSD	PDB ID	Affinity	RMSD
4IW2	-11.3	0.00	4EMX	-10.7	0.37	2BXC	-10.5	0.55
1E78	-10.9	0.36	4LB2	-10.7	0.32	2BXD	-10.5	0.55
3LU6	-10.8	1.95	1E7A	-10.6	0.45	1GNI	-10.4	2.06
2BXF	-10.7	0.45	2BXH	-10.6	0.36	3JRY	-10.4	0.30
2BXG	-10.7	0.69	2BXB	-10.5	0.63	4G03	-10.4	0.45

Table S6. Total interaction energy and its components between binding residues and BAC ligand averaged over 10 ns MD simulations. All values are in kcal/mol.

Residue	Total	Electrostatic	Van der Waals
Glu153	-9.39	-8.07	-1.31
Lys199	-9.05	-7.20	-1.85
Arg222	-8.67	-7.14	-1.53
Arg257	7.45	10.63	-3.18
Arg218	-6.67	-6.08	-0.58
Ser287	-6.44	-5.61	-0.82
Ser192	-4.31	-3.30	-1.01
Leu238	-3.20	-0.56	-2.65
Lys195	-2.72	-0.52	-2.20
Leu260	-2.67	-0.37	-2.30
His288	-2.43	-2.00	-0.43
Ile290	-2.08	0.69	-2.78

His242	-2.06	-1.01	-1.05
Ala261	-1.58	-0.53	-1.05
Tyr150	-1.47	-0.28	-1.19
Ile264	-1.15	-0.17	-0.99
Leu219	-1.10	-0.26	-0.84
Glu188	-1.05	-0.99	-0.06

Table S7. Total interaction energy and its components between binding residues and DAC ligand averaged over 10 ns MD simulations. All values are in kcal/mol.

Residue	Total	Electrostatic	Van der Waals
Lys199	-9.05	-7.40	-1.65
Glu153	-8.54	-6.78	-1.76
His242	-6.32	-5.04	-1.28
Arg222	-6.03	-5.35	-0.68
Arg218	-5.61	-5.35	-0.26
Arg257	5.23	7.76	-2.52
Leu260	-4.82	-2.18	-2.64
Tyr150	-4.19	-0.86	-3.34
Ala291	-4.04	0.45	-4.49
Leu238	-3.51	-0.68	-2.83
Gln196	-2.37	-0.81	-1.56
Lys195	-2.23	-1.32	-0.91
Lys286	2.05	2.17	-0.12
Arg160	1.76	1.89	-0.13
Ser287	-1.75	-1.16	-0.59
Glu292	1.71	3.51	-1.80
His288	-1.58	0.18	-1.76
Ser192	-1.51	-0.33	-1.19
Lys262	1.38	1.47	-0.10
Leu219	-1.35	-0.27	-1.08
Ile290	-1.18	0.95	-2.13
Glu188	-1.17	-0.91	-0.26
Leu234	-1.12	-0.13	-0.99
Phe149	-1.10	0.15	-1.26

Table S8. Calculated B3LYP/6-31G*/PCM electric dipole moment of BAC and DAC in their HSA-bonded geometry as predicted from docking simulations. Values in parenthesis were obtained after energy minimization of each structure to its nearest point on the QM landscape.

	$\lvert\mu\rvert$	μ_x	μ_y	μ_z
BAC	9.80 (11.31)	0.75 (3.66)	7.50 (7.62)	-6.27 (-7.52)
DAC	8.83 (15.36)	0.04 (-5.55)	3.40 (0.76)	-8.15 (-14.30)